

## SUPPORTING INFORMATION

### Photoelectrochemical immunoassay of aflatoxin B<sub>1</sub> in foodstuff based on amorphous TiO<sub>2</sub> and CsPbBr<sub>3</sub> perovskite nanocrystals

Lingshan Su <sup>a</sup>, Ping Tong <sup>a</sup>, Lijia Zhang <sup>a</sup>, Zhongbin Luo <sup>a</sup>, Caili Fu <sup>a</sup>, Dianping Tang <sup>a,\*</sup>, Yuyu Zhang <sup>b,\*\*</sup>

<sup>a</sup> College of Biological Sciences and Engineering, Testing Center & Key Laboratory for Analytic Science of Food Safety and Biology (MOE & Fujian Province), Department of Chemistry, Fuzhou University, Fuzhou, 350108, China

<sup>b</sup> School of Food and Chemical Engineering, Beijing Technology and Business University, Beijing, 100048, China

---

\* Corresponding author.

\*\* Corresponding author.

*E-mail addresses:* [dianping.tang@fzu.edu.cn](mailto:dianping.tang@fzu.edu.cn) (D. Tang), [zhangyuyu@btbu.edu.cn](mailto:zhangyuyu@btbu.edu.cn) (Y. Zhang).

### S1.1. Calculation Method for *t*-Test Statistics

To investigate the method accuracy between two methods, statistical comparison based on the experimental results was carried out with an unpaired Student's *t*-test. The statistics for each sample were calculated by using independent two-sample *t*-test with equal sample sizes and equal variance as follows:

$$t = \frac{|\bar{x}_1 - \bar{x}_2|}{S_{x1x2}} \sqrt{\frac{3}{2}}$$

Where

$$S_{x1x2} = \sqrt{\frac{S_{x1}^2 + S_{x2}^2}{2}}$$

The  $\bar{x}$ ,  $S_x$ , and  $n$  represent the mean, standard deviation and times of parallel detection of the samples (1, 2 mean the data obtained from the proposed method and referenced method), respectively.

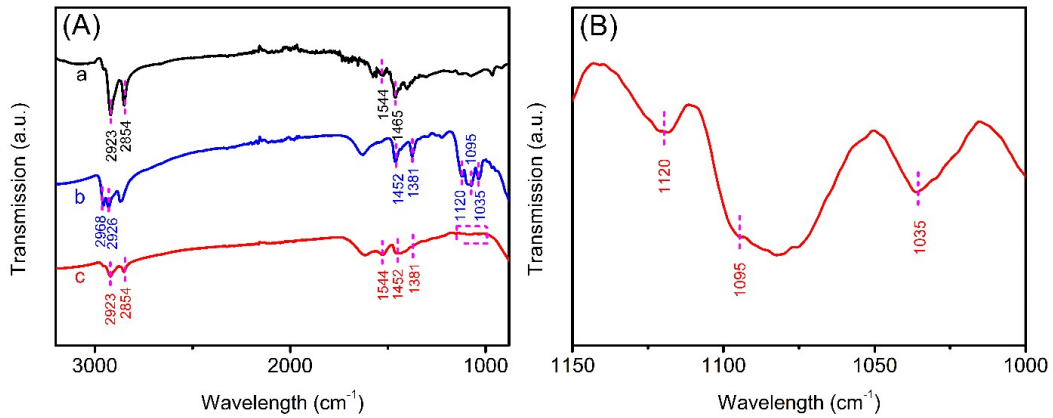


**Fig. S1.** (A) FTIR spectra of (a) CsPbBr<sub>3</sub> nanocrystals, (b) a-TiO<sub>2</sub>, and (c) CsPbBr<sub>3</sub>/a-TiO<sub>2</sub> nanocomposites; (B) the magnified FTIR spectra of CsPbBr<sub>3</sub>/a-TiO<sub>2</sub> nanocomposites.

As depicted from curve 'a' in Fig. S1, the peaks at 2923, 2854, and 1465 cm<sup>-1</sup> could be assigned to the C-H asymmetric stretching vibrations, symmetric stretching vibrations, and in-plane bending vibration, respectively. And the peak at 1544 cm<sup>-1</sup> could be contributed to the N-H bending vibration, which is a characteristic band for OAm, confirming the presence of OAm. In the case of pure a-TiO<sub>2</sub> (Fig. S1A, curve 'b'), the bands centered at 1381, 1452, 2926, and 2968 cm<sup>-1</sup> were attributed to the

bending vibrations of the  $-\text{CH}_3$  and  $-\text{CH}_2$  groups. And three characteristic absorption peaks in 1035, 1095, and  $1120\text{ cm}^{-1}$  were contributed to the Ti-O-C vibration (Fig. S1B). The main peaks were all appeared in the  $\text{CsPbBr}_3/\text{a-TiO}_2$  nanocomposites, preliminarily confirming that the obtained composites contain two fundamental components of  $\text{CsPbBr}_3$  and  $\text{a-TiO}_2$ .

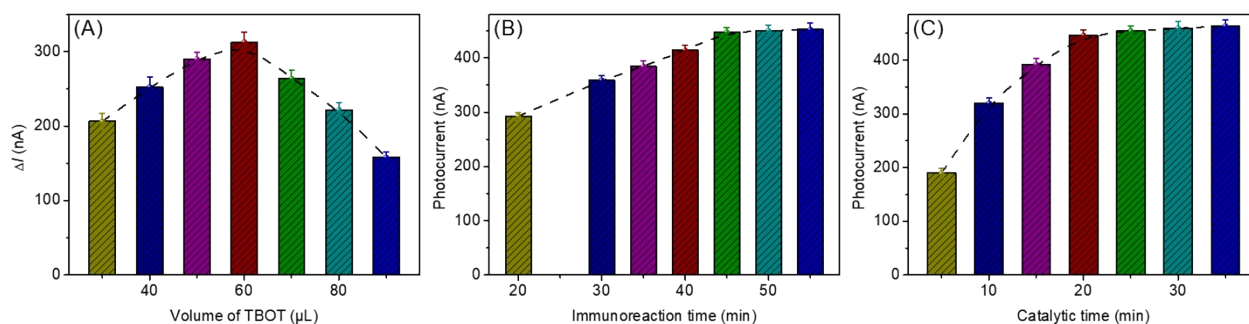


**Fig. S2.** Effects of (A) volume of TBOT, (B) the competitive immunoreaction time, and (C) the catalytic time (note:  $0.1\text{ ng mL}^{-1}$   $\text{AFB}_1$  used in the cases, and the error bars represent the standard deviation of three measurements.).

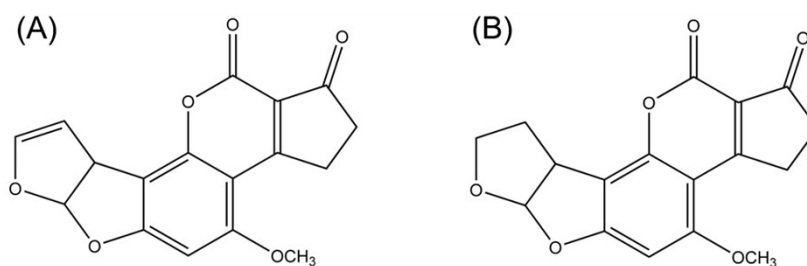


**Fig. S3.** Structures of (A)  $\text{AFB}_1$  and (B)  $\text{AFB}_2$ .

## References

- 1 Z. Li, E. Hofman, J. Li, A. Davis, C. Tung, L. Wu and W. Zheng, *Adv. Funct. Mater.*, 2018, **28**, 1704288.
- 2 Z. Li, Y. Zhu, J. Wang, Q. Guo and J. Li, *Ceram. Int.*, 2015, **41**, 9057-9062.
- 3 A. Pan, B. He, X. Fan, Z. Liu, J. Urban, A. Alivisatos, L. He and Y. Liu, *ACS Nano*, 2016, **10**, 7943-7954.
- 4 Q. Zhong, M. Cao, H. Hu, D. Yang, M. Chen, P. Li, L. Wu and Q. Zhang, *ACS Nano*, 2018, **12**, 8579-8587.